https://doi.org/10.5194/nhess-2020-127
Preprint. Discussion started: 27 April 2020

Natural Hazards and Earth System Sciences
Open Access
Discussions

Exploring the potential relationship between the occurrence of landslides and debris flows: A new approach

Zhu Liang[1], Changming Wang[1] and Kaleem Ullah Jan Khan[1]

(College of Construction Engineering, Jilin University, 130000 Changchun, People's Republic of China)

E-mail:wangcm@jlu.edu.cn

Abstract: The aim of the present study is to explore the potential relationship between landslides and debris flows by establishing susceptibility zoning maps separately with the use of random forest. Longzi township, Longzi County, located in Southeastern Tibet, where historical landslide and debris flow are commonly occurred, was selected as the study area. The work has been carried out with the following steps: **(1)** A complete landslide and debris flow inventory map was prepared; **(2)** Slope units and 11 controlling factors were prepared for the susceptibility modelling of landslide while watershed units and 12 factors for debris flow; **(3)** Establishing susceptibility zoning maps for landslide and debris flow, respectively, with the use of random forest; **(4)** The performance of two models are verified using ROC curve, the values of AUC and contingency tables; **(5)** Putting the high or very-high-class watershed units in the debris flow susceptibility zone map as the base map to observe its coverage by slope units of different classes; **(6)** The landslide zoning map was put at the bottom floor and analyzed the distribution of high or very-high-class slope units in watershed units; **(7)** transforming the slope units into points and distributed them on the watershed units. Two models based on random forest have demonstrated great predictive capabilities, of which accuracy was close to 90% and the AUC value was close to 1. The loose sources carried out by the debris flows are not necessarily brought by the landslides although most landslides can be converted into debris flows. The area prone to debris flow does not promote the occurrence of landslides. A susceptibility zoning map composed of two or more natural disasters is comprehensive and significant in this regard.

Key words: Landslide; Debris flow; Susceptibility; Random forest; Potential relationship

1. Introduction

Landslides and debris flows are natural phenomenon mainly occurring in mountainous areas, which pose considerable threats to people, industries, and the environment directly or indirectly. Generally, damages can be decreased to a certain extent by predicting the likely location of future disasters (Pradhan, 2010). Thus, extensive research has been conducted for the prediction and susceptibility assessment of landslides and debris flows.

In geomorphology, a "landslide" is the movement of a mass of rock, debris or earth down a slope, under the influence of gravity (Cruden and Varnes, 1996). Debris flow is a specific type of landslide, which can be defined as (Hungr et al. 2013): ''Very rapid to extremely rapid surging flow of saturated debris in a steep channel". Generally, a landslide that occurs on a steep slope and becomes disaggregated as it tumbles down can transform into a debris flow if it contains sufficient water for saturation. Therefore, landslide provides sufficient material source for the occurrence of debris flow and most of the landslides were accompanied by debris flow. In the past, few scholars have not been specifically distinguished the landslide and debris flow in terms of susceptibility

https://doi.org/10.5194/nhess-2020-127
Preprint. Discussion started: 27 April 2020

evaluation (Alessandro et al., 2015; Guzzetti et al., 2005). In addition, some scholars made separate evaluations of landslide and debris flow (Park et al., 2011; Haydar et al., 2016). Some scholars have proposed a coupled model of landslide-debris flow (Chiang et al., 2012; Gomes et al., 2013). However, not every landslide has evolved into a debris flow and the material source of the debris flow is may not a landslide. The causes and manifestations of landslides and debris flows are different. In a debris flow, it is possible to distinguish initiation (source area), transport and deposition zone. In other words, there is no necessary connection between debris flow and landslides. Besides, the conditioning factors and mapping units involved in the susceptibility assessment of debris flow and landslide are not identical. Therefore, it is more reasonable to evaluate the susceptibility of landslide and debris flow separately. As an example, a landslide inventory map includes only landslides, as does debris flow.

The methods of susceptibility assessment can be broadly classified as qualitative or quantitative(Aleotti et al., 1999). Several methods and approaches have been proposed and tested to ascertain susceptibility, such as physical-based approaches (Carrara et al., 2008), heuristic methods (Blais et al., 2016) and statistically-based approaches (Reichenbach et al., 2018). In addition, new machine learning models, such as neural networks (Park et al.,2013), support vector machines (Colkesen et al.,2016) and random forest (RF) (Liu et al., 2018), have also been applied.

The Longzi County in Southeastern Tibet is always exposed to landslide and debris flow hazard because of climatic and topographic conditions, which is chosen as the study area. The purpose of the present study is to explore the potential relationship between the occurrence of landslides and debris flows by establishing susceptibility zoning maps separately with the use of random forest.

2. Materials

2.1 Study area

The study area located in Longzi Township, Longzi County, Southeastern Tibet is bounded by longitudes of 92°15'E and 92°45'E, latitudes of 28°10'N and 28°30'N (Fig.1). It covers an area of about 535 km^2 with a population of more than 6000. The study area belongs to a semi-arid temperate monsoon climate with the annual rainfall of 279 mm, mainly concentrated in May to September. The seismic intensity within the area has a degree of VIII on the modified Mercalli index.

The study area belongs to the zone of stratigraphic division of the Northern Himalayan block. The strata is mainly composed of Mesozoic Cretaceous, Jurassic, Triassic, and Cenozoic units. There were three common lithology observed during our field investigation: Siltstone from the Laka Formation (K_1l); Conglomerates from the Weimei Formation (J_3w) and Quaternary slope wash (Q_4^{el+dl}) from the Cenozoic strata.

The disasters in the study area mainly consist of rain-fed high frequency debris flows and landslides, which destroyed and flooded roads, bridges, farmlands, villages, etc., causing great economic losses.

2.2 Landslide and debris flow inventory

The statistically-based susceptibility models are based on an important assumption: future landslides will be more likely to occur under the conditions which led to the landslides past and

https://doi.org/10.5194/nhess-2020-127
Preprint. Discussion started: 27 April 2020

present (Varnes, 1984; Furlani and Ninfo, 2015). Therefore, a complete and accurate inventory map is the key for model training and validation. In this study, data comes from historical records, field surveys (**Fig.2 and Fig.3**) and interpretation of Google Earth images carried out in Google Earth pro 7.1(**Fig.4**). Finally, a total of 396 landslide points and 49 debris flow points were recorded and mapped (**Fig.1**).

2.3 Mapping units

The selection of the mapping unit is an important pre-requisite for susceptibility modelling (Guzzetti, 2006). The main mapping units commonly used for landslide and debris flow susceptibility assessment are grid cells (Reichenbach et al., 2018). Despite its popularity and operational advantages, grid-cells have clear drawbacks for susceptibility modelling (Guzzetti et al., 1999). There is no physical relationship between a grid-cell, while slope units can make up for this deficiency. Depending on the landslide type, a slope unit may correspond to an individual slope, an ensemble of adjacent slopes or a small catchment (Reichenbach et al., 2018). The geometry of debris flow is better represented by apolygon or a set of polygons in vector format. In the present study, adjacent slope units were applied to the susceptibility assessment of landslides. First-order sub-catchments, which is also called watershed unit, was applied to the susceptibility of debris flow (Francesco et al., 2015; Qin et al.,2018). Therefore, ArcGIS is used in this paper to divide the study area into 174 catchments or 1003 slope units and make artificial corrections according to remote sensing image.

2.4 Controlling factors and mapping

The selection of evaluation parameters is another key prerequisite to ensure that the model is

https://doi.org/10.5194/nhess-2020-127
Preprint. Discussion started: 27 April 2020

accurate and reasonable. With reference to previous studies (Ahmed et al., 2016; Xu et al., 2013; Braun et al., 2018), there are differences in the controlling parameters used in landslide and debris flow susceptibility assessment. The occurrence of debris flow emphasizes the indispensability of provenance, topography and triggering factors. Availability, reliability, and practicality of the factor data were also considered (van Westen et al., 2008). In this paper, 11 landslide controlling factors are selected, including distance to fault, distance to road, distance to river, annual rainfall, slope angle, aspect, plan curvature, profile curvature, topographic wetness index, elevation and maximum elevation difference. Besides, a total of 12 controlling factors, including basin area, main channel length normalized difference vegetation index (NDVI), drainage density, roundness, melton, average gradient of main channel, slope angle, maximum elevation difference, annual rainfall, distance to fault and elevation were selected to fully reflect the characteristics of the watershed for the susceptibility assessment of debris flow.

The controlling factors in the present study can be categorized into four types: **(1)** The morphological factors (slope, aspect, plan curvature, profile curvature, roundness, melton); **(2)** Geological factors (distance to fault, basin area, main channel length, drainage density); **(3)** Topographical factors (elevation, maximum elevation difference, average gradient of main channel); **(4)** Environmental factors (annual rainfall, topographic wetness index, NDVI, distance to road, distance to river). Totally 18 factors are obtained by processing the row data in the ArcGIS 10.2 platform. Morpholigical and topographic related factors were derived from the DEM with a resolution of 30 × 30 m. Geological related factors were extracted from 1:50000 geological maps. Rainfall is one of the most important external factors inducing landslides and debris flow, which was determined by ordinary kriging interpolation in ArcGIS by collecting data of 6 precipitation stations near the area under study as a reference.

2.5 Mapping

In the current study, the maps of controlling factors were reclassified into 4 to 7 classes based on the equal spacing principle and the mean value in the unit was counted as the representative value of the unit. Aspect, which is frequently used as landslide controlling factor (Dai and Lee, 2002), was reclassified into 8 classes (**Fig.2**). Plan curvature and profile curvature were both considered and were both reclassified into six classes. Generally, faults, rivers and roads play a key role in the occurrence of landslides and were reclassified into seven classes using an interval of 1500m (**Fig.2**). Topographic wetness index was reclassified into five classes (**Fig.2**).

NDVI reflects the vegetation conditions in the area and was reclassified into 5 classes(**Fig.3**). Drainage density is the ratio of the total drainage length to the watershed area and was reclassified into six classes (**Fig.3**). Roundness refers to the ratio of the area of a basin to the area of a circle with the same circumference and was reclassified into six classes (**Fig.3**) . Melton ratio refers to the ratio of the degree of undulation in the watershed to the square root of the arithmetic area of the watershed (Melton, 1965), which is reclassified into seven classes (**Fig.3**). Considering the correlation between the two controlling factors, basin area and main channel length are represented by the same graph, which was reclassified into four classes (**Fig.3**). Average gradient of main channel , which is the ratio of the maximum elevation difference of main channel to its linear length, was reclassified into six classes (**Fig.3**).

Rainfall is the only triggering factor to be considered for both landslide and debris flow in this paper, which was reclassified into six classes (**Fig.2 and Fig.3**). Slope angle is frequently employed in both

https://doi.org/10.5194/nhess-2020-127
Preprint. Discussion started: 27 April 2020

landslide and debris flow susceptibility mapping and was reclassified into six classes (**Fig.2 and Fig.3**). Maximum elevation difference reflects the kinetic energy condition and is reclassified into 6 classes using an interval of 200m (**Fig.2 and Fig.3**). Elevation was reclassified into five classes (**Fig.2 and Fig.3**), which has also been used by many authors (Ayalew and Yamagishi, 2005; Pourghasemi et al. 2013a, b).

3. Methods

3.1 Sampling strategies and validation

Statistical models for landslide susceptibility zonation reconstruct the relationships between dependent and independent variables using training sets, and verify these relationships using validation sets (Guzzetti et al., 2006a,b), which usually implies the partitioning of the inventory in subsets. The sampling strategy affects the results of the susceptibility map (Yilmaz, 2010). Based on temporal, spatial or random criteria, the partition of landslide inventories can be made (Chung and Fabbri, 2003) and the most applied one is a one-time random selection (Reichenbach et al., 2018). In the current study, the random partition was used due to existing constrains with the temporal and the spatial partition. Therefore, sample data was divided into two parts: 70% of the data was selected as training data to create a prediction model, and the remaining 30% of the data was used for validation.

The computation of the area under the curve (AUC) is the most popular metrics to estimate the quality of model , which has been applied for ROC curves(Green and Swets, 1966). It is one of the most commonly used indicators. A typical two-entry confusion matrix, including true positives (TP), true negatives (TN), false positives (FP), and false negatives (FN), is another common index. In current study, both ROC curve and the contingency tables were used to

https://doi.org/10.5194/nhess-2020-127
Preprint. Discussion started: 27 April 2020

evaluate the susceptibility models established for landslides and debris flow.

3.2 Random Forests

Random forest (RF) is a powerful ensemble-learning method and was first introduced by Breiman (2001). RF uses the bagging technique (bootstrap aggregation) to select, at each node of the tree, random samples of variables and observations as the training data set for model calibration. Unselected cases (out of bag) are used to calculate the error of the model (OOB Error). The increase in OOB error is proportional to the importance of the predictive variable (Breiman and Cutler 2004). There are no restrictions on the types of variables, either numerical or categorical. RF has the ability to reduce errors caused by unbalanced data, which is suitable for susceptibility assessment.

In this study, the scikit-learn package (Pedregosa et al.,2011) in the programming software python version 3.7 was used for the modeling. The number of trees (k) and the number of predictive variables used to split the nodes (m) are two user-defined parameters required to grow a random forest (Ahmed et al.,2016). In order to ensure the algorithm convergence and good prediction results, the number of trees (k) has been fixed to 500 and the number of predictive variables (m) has been selected as 5 (Breiman et al.,2001).

4. Results and verification

4.1 Landslides susceptibility mapping results

In this study, the predictive accuracy, ROC curves and AUC values of the RF model using training data are showed in **Table 1** and **Fig. 4**. The RF model ensured very high TN and TP values of

92.86% and 93.57%, respectively. An AUC equals to 1 indicates perfect prediction accuracy (Vorpahl et al., 2012). The RF model has great performance in terms of AUC, with value of 0.978. Standard error (St.), confidence interval (CI) at 95% and significance (Sig.) are applied as three evaluation statistics. All these results indicate a reasonable goodness-of-fit for models with the training dataset, for which the values are reasonably small.

The task of validating the predicted results is the critical strategy in prediction models as shown in **Table 3** and (**Fig. 4**). Consequently, the values of TN and TP were 92.90% and 90.0%, respectively. It can be seen that the model has also a great performance in terms of AUC with value of 0.977. In comparison with the training model, the accuracy and AUC values have slightly decreased, but still perform well.

The landslide susceptibility map was also reclassified into five classes: very low (0~0.2), low (0.2~0.4), moderate (0.4~0.6), high (0.6~0.8), very high (0.8~1) by using the equal spacing method (**Fig.5**). The maps should satisfy two spatial effective rules: (1) The existing disaster points should belong to the high-susceptibility class and **(2)** The high-susceptibility class should cover only small areas (Bui et al. 2012). The number of units belonging to very high class reached 179, accounting for 17% (**Fig.6**). Disaster points were mostly in the dark (red or orange) areas. The units belonging to moderate class accounted for the smallest proportion, at 13% (**Fig.7**).

The controlling factors with significant effects were selected and normalized as shown in **Table 2**. The weight values of slope angle, distance to fault, plan curvature and topographic wetness index was 0.21, 0.19, 0.17, 0.13 respectively, which was closely related to the occurrence of landslide. The weight values of distance to road, maximum elevation difference, profile curvature and elevation are less than 0.1 as 0.08, 0.08, 0.06, and 0.05, respectively (**Fig.7**).

4.2 Debris flow susceptibility mapping result

The debris flow susceptibility model perform well with a very high TN and TP values as 90.90% and 91.18%, respectively. In terms of AUC, the model has also a great prediction performance with the value of 0.979 (**Fig.4**). Three evaluation statistics also indicate a reasonable goodness-of-fit for the model.

Table 1 shows that in the 30% sample data used for verification, the values of TN and TP were 89.13% and 86.67%, which were slightly decreased compared to the training model. It can be seen that the model has also a great performance in terms of AUC, with value of 0.968.

The number of units belonging to very high-class reached to 26, which is accounting for 15% while the units belonging to high-class accounted for the smallest proportion at 13%. More than half of the units (58%) belong to on a low or very low-class (**Fig.6**). Disaster points were mostly in the dark (Bright or deep red) areas (**Fig.5**).

The weight values of main channel length, roundness and slope angel were 0.25, 0.16, 0.14 respectively, which has significant influence on the occurrence of debris flow. The weight values of elevation, maximum elevation difference, melton and basin area are close to 0.1, which are 0.13, 0.12, 0.1, and 0.1 respectively(**Fig.7**).

4.3 Analysis and comparison of landslide and debris flow susceptibility

It is worth comparing the two susceptibility zonation. In terms of prediction accuracy, the values of TP, TN and AUC of landslide model are slightly higher than that of debris flow. However, both models achieved high predictive performance. Therefore, the landslide and debris flow

Natural Hazards and Earth System Sciences
Open Access
EGU
Discussions

susceptibility assessment models based on random forest are reliable. The purpose of the present study is to explore the potential relationship between landslides and debris flows by establishing susceptibility zoning maps. Figure 8 shows the overlapping distance between debris flow and landslide in high or very high-class of susceptibility areas. It can be seen from the figure that most of the areas with high or very high-class in the map of debris flow are covered with landslides. However, there are also non-overlapping areas between the two zoning maps. There are 23 units belonging to high-class in the debris flow susceptibility zoning map (**Fig.8**), of which 17 units are covered with high or very high-class units in the landslide zoning map (**Table 4**). In addition, there are 4 watershed units covered with low or very low class slope units. In the same way, 19 watershed units belonging to very high-class are covered with high or very high-class slop units and 4 watershed units with low or very low-class slop units. In other words, more than 70% of the high or very high-class watershed units are covered with high or very high-class slope units. However, there are still 30% of watershed units with high or very high-class without the distribution of slope units in corresponding grades. It validated the previous view that most of landslides can be transformed into debris flows. Factor analysis was applied to further analyze the reasons for the difference. 36 watershed units with distribution of high-grade slope units were taken as model 1 and the left 8 watershed units as model 2. The KMO (Kaiser-Meyer-Olkin) statistic test values were 0.766 and 0.643 respectively, which indicated that the correlation between variables is obvious and suitable for factor analysis (**Table 5)**. In model 1, the cumulative contribution rate of the three factors (C1, C2 ,C3) reached to 83.6%, while the cumulative contribution rate of the first four factors (F1, F2 ,F3 and F4) reached to 80.5% for model 2 (**Table 6**). According to the correlation coefficient of each common factor (**Table 6**), the first common

https://doi.org/10.5194/nhess-2020-127
Preprint. Discussion started: 27 April 2020

factor mainly highlighted the information of basin area, main channel length and maximum elevation difference. Similarly, the second and the third common factor highlighted the information of slope angle and elevation and roundness, respectively. The difference between the two models is that the second model has the fourth common factor (**Table 7**), which emphasized the effects of rainfall and distance to the fault. The transformation from a landslide to a debris flow most often occurs during heavy rainfall (Takahashi, 1978), and the landslides are the source area. But landslides are not the only source of debris flows. The loose material distributed in the basin is not necessarily caused by landslide.

In turn, we analyze the distribution of high or very high-class slope units in watershed units. The landslide zoning map was put at the bottom floor and the debris flow zoning map on the top floor (**Fig8**). There are 167 slope units belonging to high-class in the landslide susceptibility zoning map (**Fig.6**), of which 68 units (accounting for about 40%) are distributed in the area of high or very high-class watershed units in the debris flow zoning map (**Table 8**). Besides, 69 slope units (accounting for about 41%) are distributed in the area of low or very low-class watershed units. Similarly, 53 slope units (accounting for about 30%) belonging to very high-class are distributed in the area of high or very high-class watershed units and 88 slope units (accounting for about 50%) in low or very low-class slop units (**Table 8**). Comparing with the extent of the landslide affecting the debris flow, the impact of the debris flow on the landslide is not obvious. This indicates that the area prone to debris flow does not promote the occurrence of landslides.

Finally, we took the center of gravity of 1,003 slope units as the potential hazard points and spread them over 174 watershed units. Thus, a combining susceptibility prediction map for landslide and debris flow was obtained (Fig.8). The darker the color, the higher the class of

https://doi.org/10.5194/nhess-2020-127
Preprint. Discussion started: 27 April 2020

susceptibility will be. It can be seen from the figure that the level of disaster susceptibility in the south is generally higher than that in the north, and the area in the southwest is disaster-prone. The northeast and central locations in the area are less likely to be affected by disasters and belong to low-susceptibility areas. Green or yellow dots, which refer to slope units with very low or low-class in the landslide zoning map, mainly distributed in light-colored areas but there are also quite a few green or yellow dots distributed in dark areas, which means that the occurrence of debris flow not necessarily depend on landslides. Blue or black spots are mainly distributed in dark areas but there are also quite a few blue or black spots distributed in dark light areas, which means that landslide is not the only condition for debris flow to occur. Most of the watershed units are distributed with two or more colored dots, which means that there would be multiple slope units with different susceptibility class in the same watershed. According to the susceptibility zoning maps of landslide and debris flow, the study area can be divided into 4 categories: **(1)** Low or very low-class watershed units coupled with low or very low-class slope units; **(2)** Low or very low-class watershed units coupled with high or very high-class slope units; **(3)** High or very high-class watershed units coupled with low or very low-class slope units; **(4)** High or very high-class watershed units coupled with high or very high-class slope units. We assume that the occurrence of landslides can bring rich sources of debris flow, thereby promoting or aggravating the outbreak of debris flow, that is, forming a landslide-debris flow disaster chain. Therefore, the susceptibility assessment of the landslide-debris flow chain in the study area can be roughly divided into three classes, which are low, moderate and high (**Table 8**).

5. Discussion

5.1 Method used for modeling

Many researchers have used different statistically-based methods to evaluate the susceptibility of landslides or debris flows. Logistic regression and discriminant analysis are the most popular methods to use in traditional multivariate statistical analysis. The performance of new learning machines, such as support vector machines and neural networks, has also been verified. Random forest, as a newly integrated learning machine, has less application in landslide and debris flow analysis. Actually, random forests have powerful data processing capabilities and can simultaneously solve problems such as high-dimensional, unbalanced and data loss, which are common in geological disaster assessment. Most importantly, random forests can compare the important differences between features and have strong ability to resist overfitting and generalization, which is difficult to achieve by other statistical methods.

5.2 Potential relationship between landslide and debris flow

There is a certain similarity in the evaluation of the susceptibility of landslides and debris flows from the concept, the selection of controlling factors and the application of modeling strategies. Therefore, some researchers have neglected the difference between landslide and debris flow i.e to express two different disasters with the same susceptibility zoning map(Ciurleo et al., 2016; Ciurleo et al., 2017; Persichillo et al., 2017;). However, similarity does not always mean consistency. Many researchers have previously conducted studies into the debris flow mobilization from shallow landslide using a coupled methodology. They are interested in the dynamic simulation of debris flow based on the prediction of landslide susceptibility(Wang et al., 2013; Fan

https://doi.org/10.5194/nhess-2020-127
Preprint. Discussion started: 27 April 2020

Natural Hazards and Earth System Sciences
Open Access
Discussions

et al., 2017). However, not every landslide evolves into a debris flow, which means that the analysis process is highly selective or uncertain. In the same way, the source of the debris flow is not limited to landslides. Therefore, the potential relationship between landslides and debris flows needs to be discussed more reasonably and effectively. There, the potential relationship between landslides and debris flows needs to be discussed more reasonably and effectively. In this paper, the corresponding influencing factors and mapping units are selected to establish landslide and debris flow susceptibility zoning maps, respectively. The potential relationship between landslide and debris flow is explored in two ways: **1)** Superimposing the high or very high-class susceptibility areas in the two maps; **2)** Transforming the slope units into points and distributed them on the watershed units. The relationship between landslide and debris flow is illustrated by the distribution of slope units of different grades on the watershed units with different prone grades.

5.3 Necessity and feasibility of combining multiple natural disaster susceptibility zoning maps

Previous studies on susceptibility zoning mapping of disaster have agreed that one disaster corresponds to one map. Multiple disasters may be bred simultaneously in a watershed unit and it will cause some confusion in practical. For example, the probability of a disaster occurring in a watershed is negligible, while the probability of another disaster occurring is high. If so, we need to combine multiple zoning maps at the same time to give a comprehensive evaluation, which is arduous to achieve. On the one hand, the prediction accuracy and error of different zoning maps should be similar or even consistent. On the other hand, the dimensions of the mapping unit should be consistent or complementary. The fact that the appropriate prediction method and mapping units applied to the two disasters makes it possible to merge the two zoning maps .In addition, two natural disasters with potential relationship are simultaneously reflected in the same susceptibility zoning map, which can better guide the implementation of engineering, such as landslide-debris flow disaster chain.

6. Conclusion

In this paper, susceptibility prediction models for landslides and debris flows are established through random forest, respectively and the performance of the models are excellent in terms of accuracy and goodness of fit. The potential relationship between landslide and debris flow is discussed by the superimposition of two zoning maps and the following conclusions can be drawn:

(1) The landslide and debris flow susceptibility prediction models based on random forest have great performance of accuracy and goodness-of-fit and have the ability to analyze the relative importance of different impact factors, which is suitable for the evaluation of natural disasters;

(2) Although most landslides will be converted into debris flows, the landslides are not necessarily the source of debris flows, and the loose sources carried by the debris flow are not necessarily brought by the landslides;

(3) By comparing the extent of the landslide affecting the debris flow, the impact of the debris flow on the landslide is not obvious, which indicates that the area prone to debris flow does not promote the occurrence of landslides;

(4) A susceptibility zoning map composed of two or more natural disasters is more comprehensive and significant, which provides valuable reference for researchers and engineering

applications.

Data availability

The data used to support the findings of this study are included within the article.

Author contribution:

Zhu Liang was responsible for the writing and graphic production of the manuscript. Changming Wang was responsible for the revision of the manuscript. Kaleem Ullah Jan Khan was responsible for the translation.

Competing interests:

The authors declare that they have no conflict of interest.

Acknowledgements

This work was supported by the National Natural Science Foundation of China (Grant No. 4197020250).

References:

Ayalew L, Yamagishi H (2005) The Application of GIS-based logistic regression for landslide susceptibility mapping in the Kakuda–Yahiko Mountains, central Japan. Geomorphology 65:15–31. doi:10.1016/j. geomorph. 2004.06.010

Alessandro Trigila, Carla Iadanza, Carlo Esposito, et al. Comparison of Logistic Regression and Random Forests techniques for shallow landslide susceptibility assessment in Giampilieri

(NE Sicily, Italy). 2015, 249:119-136.

Ahmed Mohamed Youssef, Hamid Reza Pourghasemi, Zohre Sadat Pourtaghi, et al. Erratum to: Landslide susceptibility mapping using random forest, boosted regression tree, classification and regression tree, and general linear models and comparison of their performance at Wadi Tayyah Basin, Asir Region, Saudi Arabia. 2016, 13(5):1315-1318.

Anika Braun, Elias Leonardo Garcia Urquia, Rigoberto Moncada Lopez, et al. Landslide Susceptibility Mapping in Tegucigalpa, Honduras, Using Data Mining Methods. 2018.

Breiman, L.,2001. Random Forests. Machine learning, 45(1): 5-32. doi:https://doi.org/10.1023/A:10 1093340

Breiman L, Cutler A (2004) http://www.stat.berkeley.edu/users/Breiman/RandomForests/ccpapers.h-Tml

Bui DT, Pradhan B, Lofman O, Revhaug I, Dick OB (2012) Landslide susceptibility assessment in the Hoa Binh Province of Vietnam: a comparison of the Levenberg-Marquardt and Bayesian regularized neural networks. Geomorphology. doi:10.1016/j.geomorph.2012.04.023

Blais-Stevens A, Behnia P (2016) Debris flow susceptibility mapping using a qualitative heuristic method and flow-R along the Yukon Alaska Highway Corridor, Canada. Nat Hazard Earth Syst Sci 16(2):449–462.

Chung, C.F., Fabbri, A.G., 2003. Validation of spatial prediction models for landslide hazard mapping. Nat. Hazards 30,451–472.

Carrara A, Crosta G, Frattini P (2008) Comparing models of debris-flow susceptibility in the alpine environment. Geomorphology 94:353-378

Chunxiang Wang, Hideaki Marui, Gen Furuya, et al. Two Integrated Models Simulating Dynamic

Process of Landslide Using GIS. 2013.

Chung, C.F., Fabbri, A.G., 2003. Validation of spatial prediction models for landslide hazard mapping. Nat. Hazards 30, 451–472.

Colkesen, I., Sahin, E.K., Kavzoglu, T., 2016. Susceptibility mapping of shallow landslides using kernel-based Gaussian process, support vector machines and logistic regression. African Earth Sciences]–>J. Afr. Earth Sci. 118, 53–64.

Cruden, D.M., Varnes, D.J., 1996. Landslide types and processes. In: Turner, A.K., Schuster, R.L. (Eds.), Landslides, Investigation and Mitigation, Special Report 247. Transportation Research Board, Washington D.C., pp. 36–75 ISSN: 0360-859X, ISBN: 030906208X.

Dai, F.C., Lee, C.F., 2002. Landslide characteristics and slope instability modelling using GIS, Lantau Island, Hong Kong. Geomorphology 42, 213–228.

D. W. Park, N. V. Nikhil, S. R. Lee. Landslide and debris flow susceptibility zonation using TRIGRS for the 2011 Seoul landslide event. 2013, 13(11):2833-2849.

Furlani, S., Ninfo, A., 2015. Is the present the key to the future? Earth-Sci. Rev. 142 (C),38–46.

Francesco Bregoli, Vicente Medina, Guillaume Chevalier, et al. Debris-flow susceptibility assessment at regional scale: Validation on an alpine environment. 2015, 12(3):437-454.

Green, D.M., Swets, J.M., 1966. Signal Detection Theory and Psychophysics. John Wiley and Sons, New York ISBN: 0-471-32420-5.

Guzzetti, F., Carrara, A., Cardinali, M., Reichenbach, P., 1999. Landslide hazard evaluation: a review of current techniques and their application in a multi-scale study, Central Italy. Geomorphology 31, 181–216.

Guzzetti. F, M. Galli, P. Reichenbach, et al. Landslide hazard assessment in the Collazzone area,

https://doi.org/10.5194/nhess-2020-127
Preprint. Discussion started: 27 April 2020

Umbria, Central Italy. 2006, 6(1):115.

Guzzetti, F., Galli, M., Reichenbach, P., Ardizzone, F., Cardinali, M., 2006a. Landslide hazard assessment in the Collazzone area, Umbria, central Italy. Nat. Hazard. Earth Syst. Sci. 6, 115–131.

Guzzetti, F., Reichenbach, P., Ardizzone, F., Cardinali, M., Galli, M., 2006b. Estimating the quality of landslide susceptibility models. Geomorphology 81, 166–184.

Gomes, R. A. T., Guimaraes, R. F., Carvalho Júnior, O. A., Fernandes, N. F., and Amaral Jr., E. V.: Combining spatial models for shallow landslides and debris flows prediction, Remote Sens., 5,2219–2237, 2013

Hungr, O., Leroueil, S., Picarelli, L., 2013. The Varnes classification of landslide types, an update. Landslides 11 (2), 167–194.

Haydar Y. Hussin, Veronica Zumpano, Paola Reichenbach, et al. Different landslide sampling strategies in a grid-based bi-variate statistical susceptibility model. 2016, 253:508-523.

Lee, S., Dan, N.T., 2005. Probabilistic landslide susceptibility mapping on the Lai Chau province of Vietnam: focus on the relationship between tectonic fractures and landslides. Environmental Geology 48, 778–787.

Linfeng Fan, Peter Lehmann, Brian McArdell, et al. Linking rainfall-induced landslides with debris flows runout patterns towards catchment scale hazard assessment. 2017, 280:1-15.

Liu, Kai; Wang, Ming; Cao, Yinxue; Zhu, Weihua; Yang, Guiling., 2018. Susceptibility of existing and planned Chinese railway system subjected to rainfall-induced multi-hazards. Transportation Research Part A: Policy & PracticeVol.117 214-226

Liqiang Tong, Wensheng Qi, Guoying An,Chunling Liu. Remote sensing survey of major

https://doi.org/10.5194/nhess-2020-127
Preprint. Discussion started: 27 April 2020

geological disasters in the Himalayas[J].Journal of engineering geology,2019,27(03):496.

Melton M A． The Geomorphic and Paleoclimatic Significance of Alluvial Deposits in Southern Arizona: A Reply［J］. The Journal of Geology，1965，73(1) : 102 －106.

Mariantonietta Ciurleo, Michele Calvello, Leonardo Cascini. Susceptibility zoning of shallow landslides in fine grained soils by statistical methods. 2016, 139:250-264.

Mariantonietta Ciurleo, Leonardo Cascini, Michele Calvello. A comparison of statistical and deterministic methods for shallow landslide susceptibility zoning in clayey soils. 2017, 223:71-81.

Maria Giuseppina Persichillo, Massimiliano Bordoni, Claudia Meisina, et al. Shallow landslides susceptibility assessment in different environments. 2017, 8(2):748-771.

P. Aleotti, R. Chowdhury. Landslide hazard assessment: summary review and new perspectives. 1999, 58(1):21-44.

Pradhan, B., 2010. Landslide susceptibility mapping of a catchment area using frequency ratio, fuzzy logic and multivariate logistic regression approaches. J. Indian Soc. Remote Sens. 38 (2), 301–320.

Pedregosa,F., Varoquaux,G., Gramfort, A., et al., 2011. Scikit-Learn: Machine Learning in Python. Journal of machine learning research, 12(10): 2825-2830.

P. Vorpahl, H. Elsenbeer, M. Märker, and B. Schröder, "How can statistical models help to determine driving factors of landslides?" Ecol. Model., vol. 239, pp. 27–39, 2012

Pourghasemi HR, Moradi HR, Fatemi Aghda SM (2013a) Landslide susceptibility mapping by binary logistic regression, analytical hierarchy process, and statistical index models and assessment of their performances. Nat Hazards 69:749–779. doi:10.1007/s11069-013-0728-5

https://doi.org/10.5194/nhess-2020-127
Preprint. Discussion started: 27 April 2020

Pourghasemi HR, Pradhan B, Gokceoglu C, Mohammadi M, Moradi HR (2013b) Application of weights-of-evidence and certainty factor models and their comparison in landslide susceptibility mapping at Haraz watershed, Iran. Arab J Geosci 6(7):2351–2365. doi:10.1007/s12517-012-0532-7

Reichenbach,P.,Rossi,M.,Malamud,B.D.,et al.,2018.A Review of Statistically-Based Landslide Susceptibility Models. Earth-Science Reviews, 180(5): 60-91. doi:https://doi.org/10.1016/j.earscirev. 2018. 03. 001

Shou-Hao Chiang, Kang-Tsung Chang, Alessandro C. Mondini, et al. Simulation of event-based landslides and debris flows at watershed level. 2011, 138(1):306-318.

Shengwu Qin, Jiangfeng Lv, Chen Cao, et al. Mapping debris flow susceptibility based on watershed unit and grid cell unit: a comparison study. 2019, 10 (1):1648-1666.

Takahashi, T., 1978. Mechanical characteristics of debris flow. Journal of the Hydraulics Division 104, 1153–1169.

Varnes, D.J., IAEG Commission on Landslides and other Mass-Movements, 1984. Landslide Hazard Zonation: A Review of Principles and Practice. The UNESCO Press, Paris (63 pp).

van Westen CJ, Castellanos E, Kuriakose SL (2008) Spatial data for landslide susceptibility, hazard, and vulnerability assessment: an overview. Eng Geol 102(3–4):112–131

Xu WB, Yu WJ, et al. (2013) Debris flow susceptibility assessment by GIS and information value model in a large-scale region, Sichuan Province (China).Natural Hazards 65(3):1379-1392.

Yilmaz, I., 2010. The effect of the sampling strategies on the landslide susceptibility mapping by conditional probability and artificial neural networks. Environ. Earth Sci. 60,505–519.

https://doi.org/10.5194/nhess-2020-127
Preprint. Discussion started: 27 April 2020

Natural Hazards and Earth System Sciences
Discussions

Table 1 The prediction accuracy of RF

	70%			30%			100%		
Test group	Total	TN	TP	Total	TN	TP	Total	TN	TP
Landslide (%)	93.14	92.86	93.57	91.75	92.90	90.00	92.72	92.87	92.50
Debris flow (%)	90.98	90.91	91.18	88.46	89.19	86.67	89.08	88.80	89.80

Table 2 Controlling factors assigned by the RF

Test group	Slope angle	Distance to fault	Plan curvature	Topographic wetness index	Distance to road	Maximum elevation difference	Profile curvature	Elevation
Landslide	0.21	0.19	0.17	0.13	0.08	0.07	0.06	0.05

Table 3 Controlling factors assigned by the RF

Test group	Main channel length	Roundness	Slope angle	Elevation	Maximum elevation difference	Melton	Basin area
Debris flow	0.25	0.16	0.14	0.13	0.12	0.1	0.1

Table 4 The overlap number of debris flow and landslide height and very high-class mapping units

Debris flow \ Landslide	Very low	Low	High	Very high
High	3/23	1/23	5/23	12/23
Very high	2/26	2/26	8/26	11/26

https://doi.org/10.5194/nhess-2020-127
Preprint. Discussion started: 27 April 2020

Table 5 Statistical variables of the two models

Model / Statistical variables	Model 1	Mode 2
KMO	0.766	0.643
Sig.	0.001	0.003

Table 6 The correlation coefficients between common factors and primitive variables

Factor	F1	F2	F3
NDVI	0.386	-0.336	-0.621
Basin area	0.897	-0.007	0.041
Main channel length	0.984	0.046	-0.023
Slop angle	-0.223	0.829	0.455
Maximum elevation difference	0.744	0.66	0.011
Rainfall	-0.768	0.33	0.201
Average gradient of main channel	-0.753	0.544	0.106
Drainage density	-0.844	0.06	0.015
Roundness	0.331	0.14	0.818
Elevation	0.133	0.846	0.382
Distance to fault	-0.16	0.211	0.421
Melton	-0.625	0.737	0.149
Contribution rate (%)	41.2	24.7	16.7

Natural Hazards and Earth System Sciences
Discussions

Accumulative contribution (%)	41.2	65.9	83.6

497

498 **Table 7** The correlation coefficients between common factors and primitive variables

Factor	C1	C2	C3	C4
NDVI	0.042	-0.079	-0.279	-0.813
Basin area	0.802	-0.344	0.057	0.009
Main channel length	0.885	0.126	-0.196	0.227
Slop angle	0.009	0.748	0.58	-0.057
Maximum elevation difference	0.801	0.434	-0.128	0.144
Rainfall	0.197	-0.076	-0.487	0.637
Average gradient of main channel	-0.744	0.205	0.15	-0.23
Drainage density	-0.776	-0.176	-0.267	0.117
Roundness	-0.014	0.022	0.896	-0.002
Elevation	0.34	0.746	0.25	0.326
Distance to fault	0.31	0.289	-0.344	0.757
Melton	-0.182	0.932	-0.192	0.061
Contribution rate (%)	29.2	20.3	15.2	15.8
Accumulative contribution (%)	29.2	49.5	64.7	80.5

499 **Table 8** The overlap number of landslide and debris flow height and very-high class mapping units

Debris flow / Landslide	Very low	Low	High	Very high

https://doi.org/10.5194/nhess-2020-127
Preprint. Discussion started: 27 April 2020

High	36/167	33/167	25/167	43/167
Very high	48/179	40/179	25/179	28/179

Table 9 Comprehensive evaluation of landslide-debris flow susceptibility

Landslide \ Debris flow	Low or Very low	High or Very high
Low or Very low	Low	Moderate
High or Very high	Moderate	High

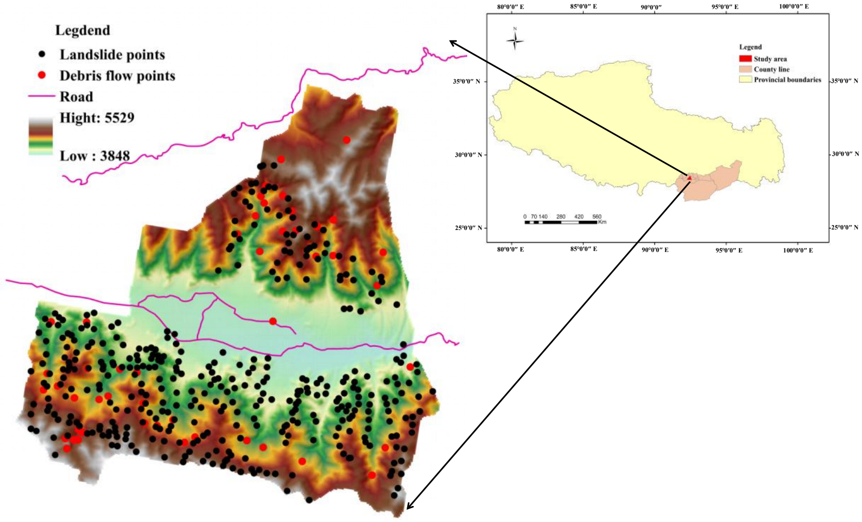

Fig.1. Location map of the study area showing landslide and debris flow inventory.

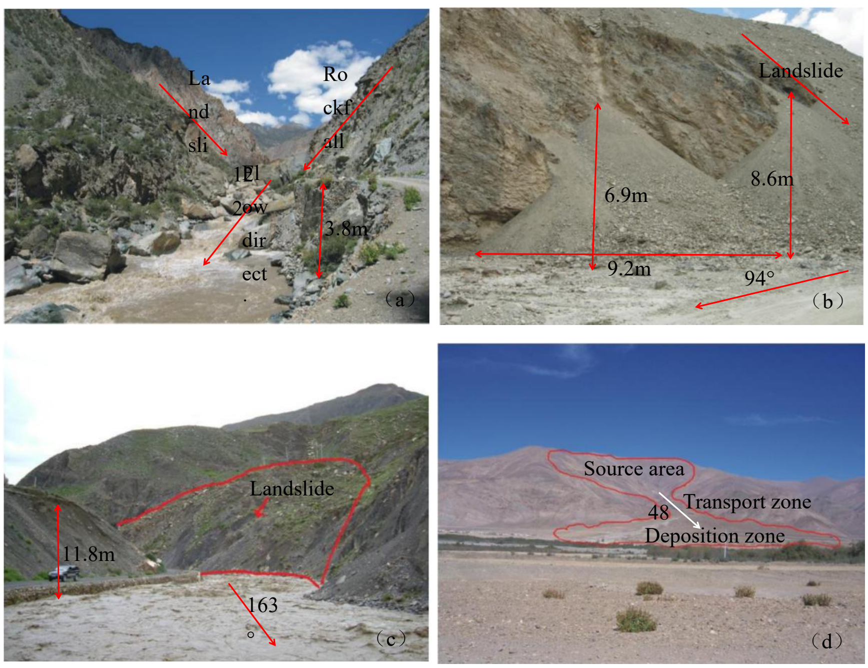

Fig.2. Photos of landslide or debris flow: (a) Lunba landslide in a tributary; (b) Zhenqiong landslide in Jiayu village; (c) Debris flow in Misha Township; (d) Debris flow in Lelong Village.

https://doi.org/10.5194/nhess-2020-127
Preprint. Discussion started: 27 April 2020

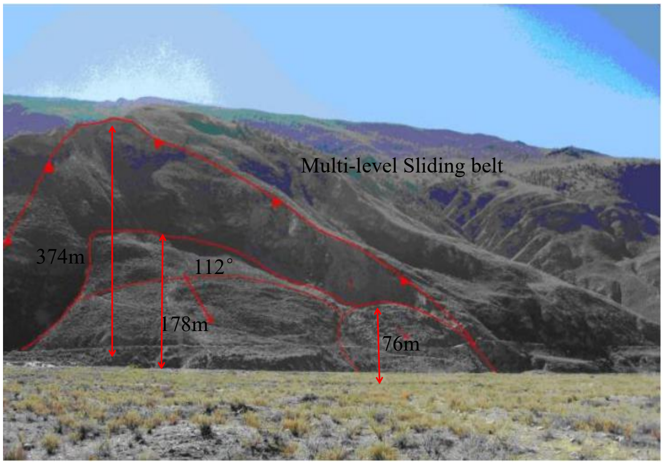

Fig.3. Multistage landslide in Xiongqu village

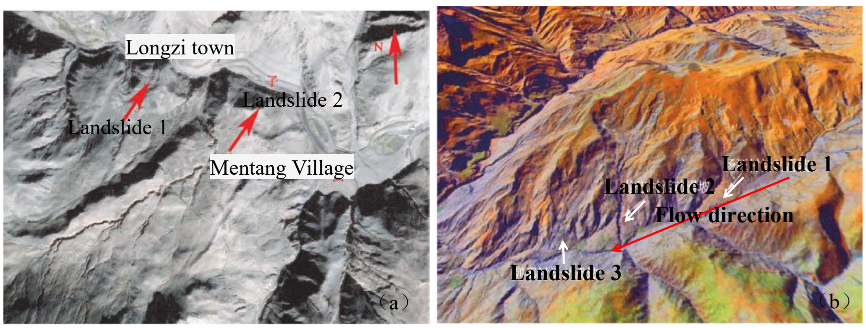

Fig.4. Stereo remote sensing map of landslides in Longzi Township (Tong et al., 2019)

https://doi.org/10.5194/nhess-2020-127
Preprint. Discussion started: 27 April 2020

Natural Hazards and Earth System Sciences
Open Access
Discussions

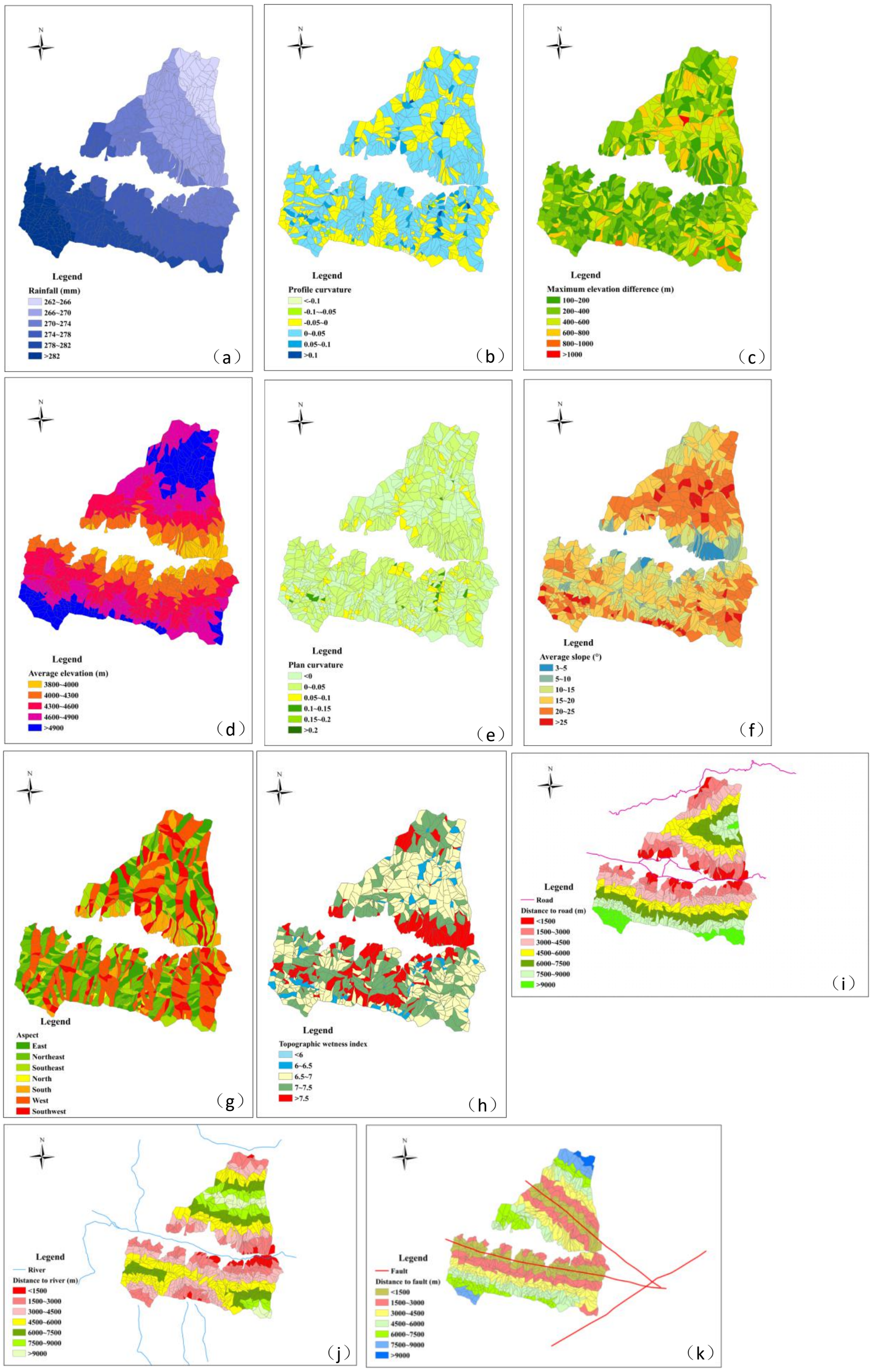

Fig.5. Study area thematic maps for landslide:（**a**）Rainfall;（**b**）Profile curvature;（**c**）Maximum elevation difference;（**d**）Average elevation;（**e**）Plan curvature;（**f**）Average slope;（**g**）Aspect;（**h**）Wetness;（**i**）Distance to road;（**j**）Distance to river;（**k**）Distance to fault.

https://doi.org/10.5194/nhess-2020-127
Preprint. Discussion started: 27 April 2020

Natural Hazards and Earth System Sciences
Discussions

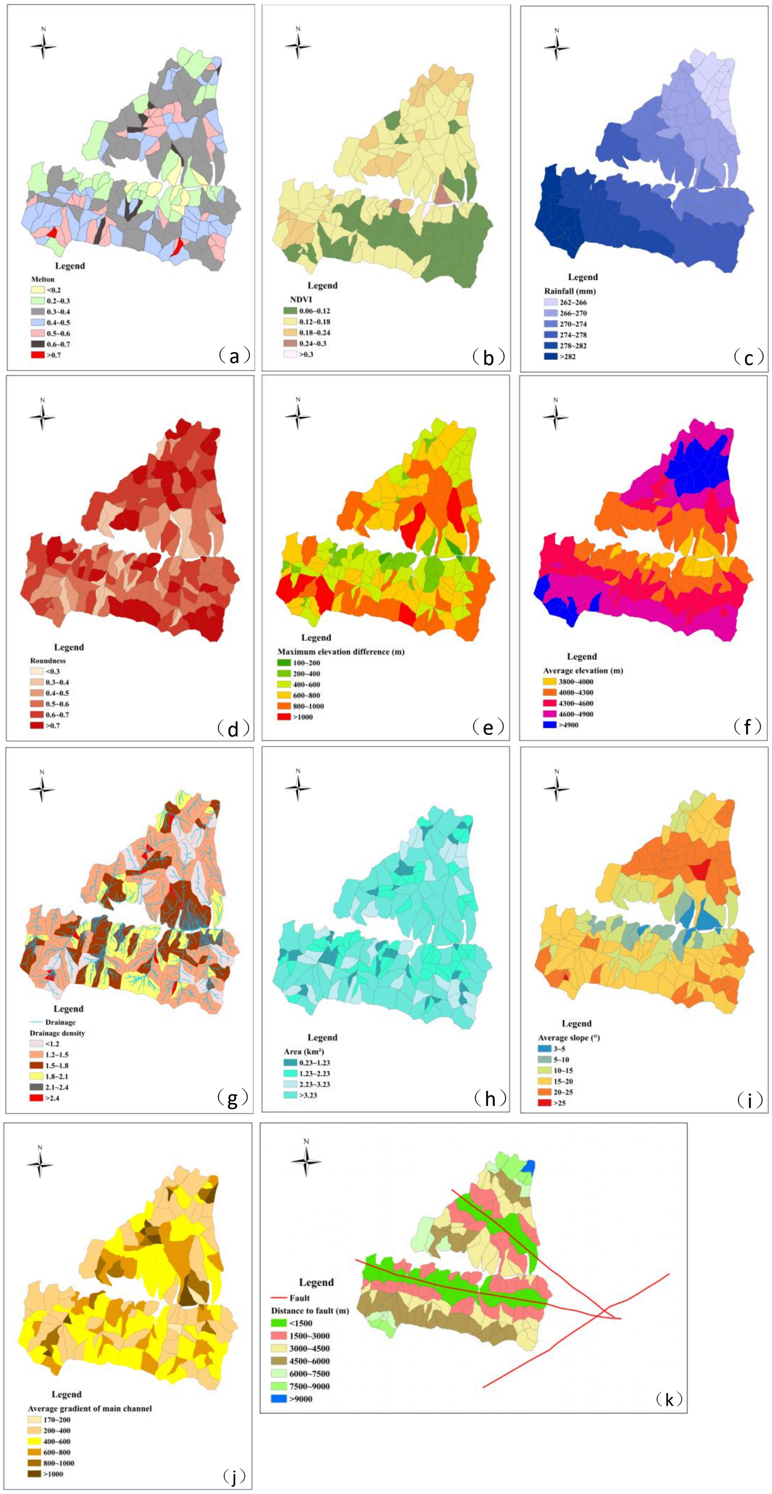

https://doi.org/10.5194/nhess-2020-127
Preprint. Discussion started: 27 April 2020

Natural Hazards and Earth System Sciences
Open Access
Discussions

Fig.6. Study area thematic maps for debris flow: (**a**) Melton; (**b**) NDVI; (**c**) Rainfall; (**d**) Roundness; (**e**) Maximum elevation difference; (**f**) Average elevation; (**g**) Drainage density; (**h**) Area; (**i**) Average slope; (**j**) Average gradient of main channel; (**k**) Distance to fault.

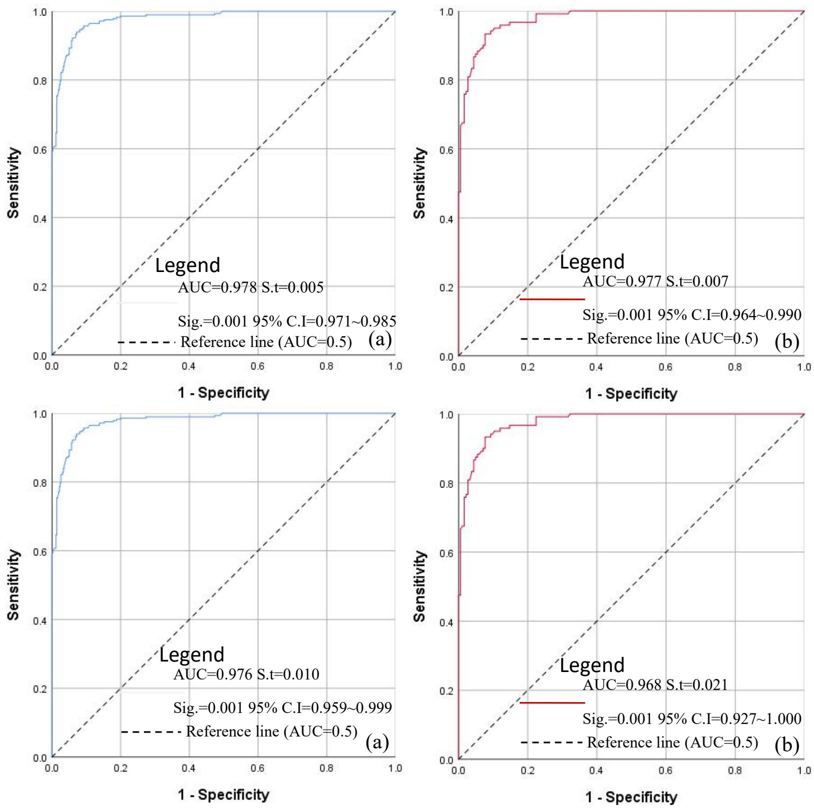

Fig.7. Analysis of ROC curve for the two susceptibility maps: **(a)** Success rate curve of landslide using the training dataset; **(b)** Prediction rate curve of landslide using the validation dataset; **(c)** Success rate curve of debris flow using the training dataset; **(d)** Prediction rate curve of debris flow using the validation dataset.

https://doi.org/10.5194/nhess-2020-127
Preprint. Discussion started: 27 April 2020

Natural Hazards and Earth System Sciences Discussions
Open Access

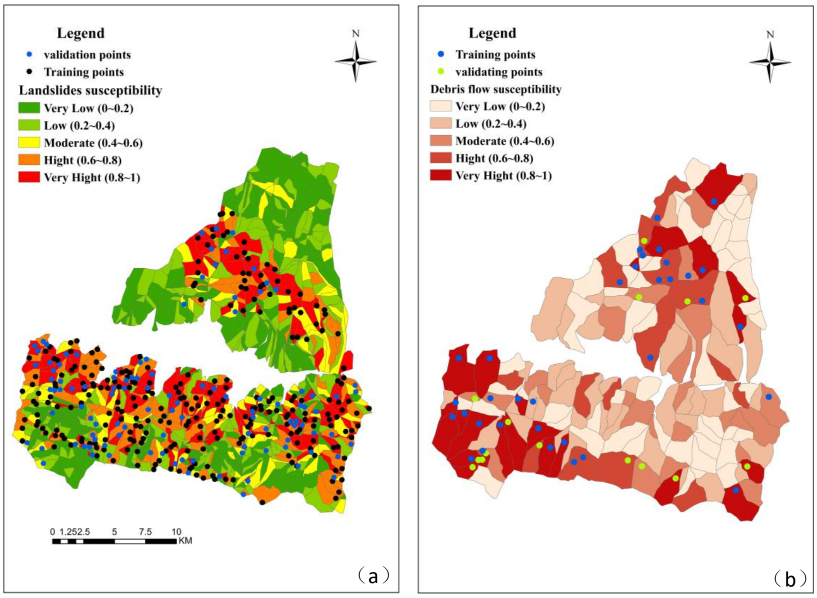

Fig.8. Susceptibility maps:（**a**）Landslide susceptibility zoning map;（**b**）Debris flow susceptibility zoing map.

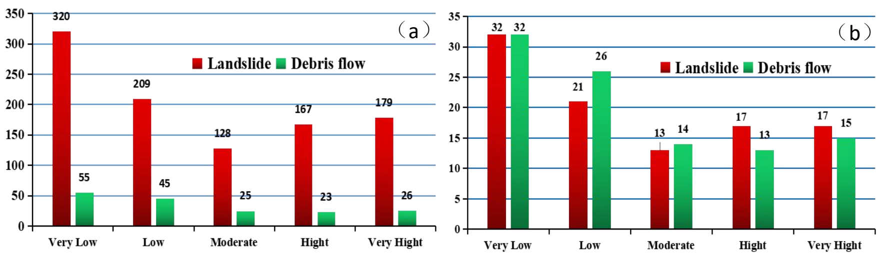

Fig.9. Numbers and percentage of units in different susceptibility classes for landslide and debris flow: **(a)** Numbers of units in different susceptibility classes for landslide and debris flow; **(b)** Percentages of different susceptibility classes for landslide and debris flow.

https://doi.org/10.5194/nhess-2020-127
Preprint. Discussion started: 27 April 2020

Natural Hazards and Earth System Sciences
Open Access
Discussions

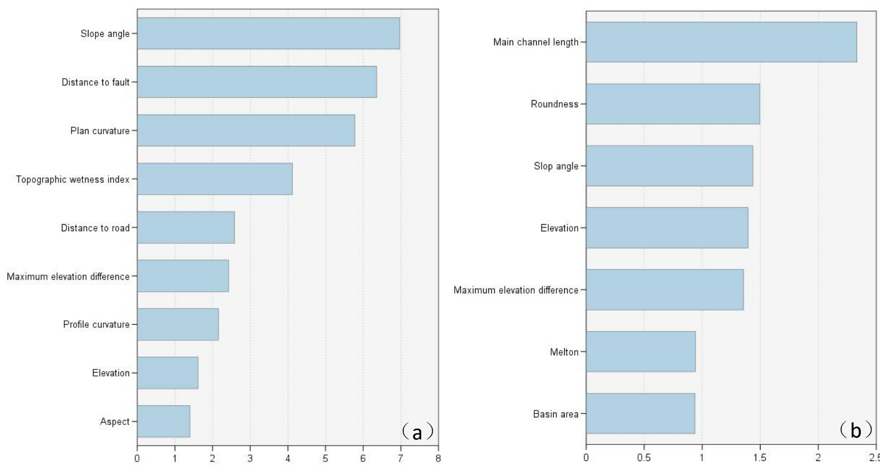

Fig.10. Parametric importance graphics obtained from RF model: **(a)** Parametric importance graphics of landslide; **(b)** Parametric importance graphics of debris flow.

Natural Hazards and Earth System Sciences
Open Access
EGU
Discussions

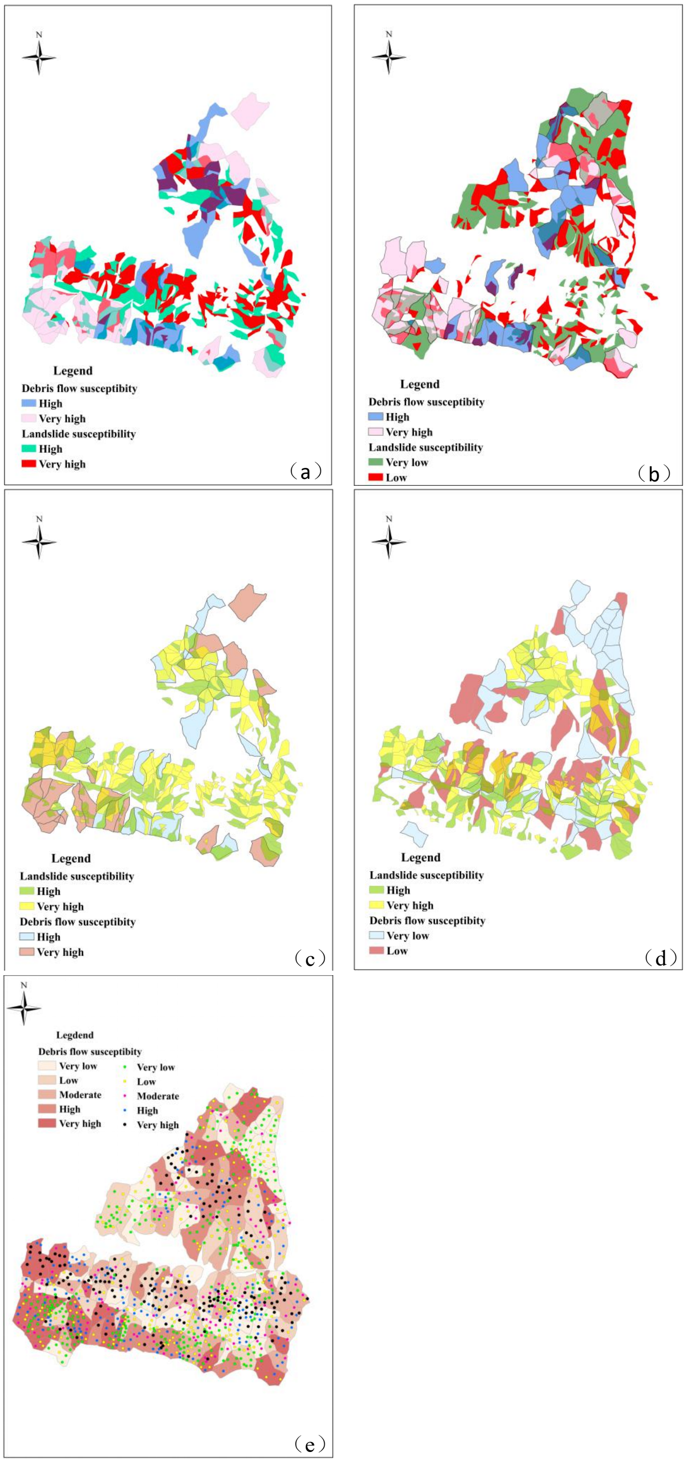

https://doi.org/10.5194/nhess-2020-127
Preprint. Discussion started: 27 April 2020

Natural Hazards and Earth System Sciences Discussions
Open Access

Fig.11. Landslide-debris flow susceptibility maps: **(a)** Height and very high-class watershed units with high or very high slope units; **(b)** High or very high-class watershed units with low or very low slope units; **(c)** High or very high-class slope units with high or very high-class watershed units; **(d)** Mapping units.